Published in final edited form as:
Steroids. 2012 April ; 77(5): 477–483. doi:10.1016/j.steroids.2012.01.007.

A local effect of CYP24 inhibition on lung tumor xenograft exposure to 1,25-dihydroxyvitamin D_3 is revealed using a novel LC-MS/MS assay

Jan H. Beumer[a,b], **Robert A. Parise**[a,b], **Beatriz Kanterewicz**[c], **Martin Petkovich**[d], **David Z. D'Argenio**[e], and **Pamela A. Hershberger**[c,f]

[a]Molecular Therapeutics/Drug Discovery Program, University of Pittsburgh Cancer Institute, Pittsburgh, PA 15213

[b]Department of Pharmaceutical Sciences, University of Pittsburgh School of Pharmacy, Pittsburgh, PA 15213

[c]Lung and Thoracic Malignancies Program, University of Pittsburgh Cancer Institute, Pittsburgh, PA 15213

[d]Cytochroma, Markham, Ontario and Cancer Research Institute, Queen's University, Kingston

[e]Department of Biomedical Engineering, University of Southern California, Los Angeles, CA 90089

[f]Department of Pharmacology and Chemical Biology, University of Pittsburgh School of Medicine, Pittsburgh, PA 15213

Abstract

The vitamin D_3 catabolizing enzyme, CYP24, is frequently over-expressed in tumors, where it may support proliferation by eliminating the growth suppressive effects of 1,25-dihydroxyvitamin D_3 ($1,25(OH)_2D_3$). However, the impact of *CYP24* expression in tumors or consequence of CYP24 inhibition on tumor levels of $1,25(OH)_2D_3$ *in vivo* has not been studied due to the lack of a suitable quantitative method. To address this need, an LC-MS/MS assay that permits absolute quantitation of $1,25(OH)_2D_3$ in plasma and tumor was developed. We applied this assay to the H292 lung tumor xenograft model: H292 cells eliminate $1,25(OH)_2D_3$ by a CYP24-dependent process *in vitro*, and $1,25(OH)_2D_3$ rapidly induces *CYP24* expression in H292 cells *in vivo*. In tumor-bearing mice, plasma and tumor concentrations of $1,25(OH)_2D_3$ reached a maximum of 21.6 ng/mL and 1.70 ng/mL respectively, following intraperitoneal dosing (20 μg/kg $1,25(OH)_2D_3$). When co-administered with the CYP24 selective inhibitor CTA091 (250 μg/kg), $1,25(OH)_2D_3$ plasma levels increased 1.6-fold, and tumor levels increased 2.6-fold. The tumor/plasma ratio of $1,25(OH)_2D_3$ AUC was increased 1.7-fold by CTA091, suggesting that the inhibitor increased the tumor concentrations of $1,25(OH)_2D_3$ independent of its effects on plasma disposition. Compartmental modeling of $1,25(OH)_2D_3$ concentration *versus* time data confirmed that: $1,25(OH)_2D_3$ was eliminated from plasma and tumor; CTA091 reduced the elimination from

Corresponding Author Current Address: Pamela A. Hershberger; Ph.D., Roswell Park Cancer Institute, Center for Genetics and Pharmacology, L4-317, Elm and Carlton Streets, Buffalo, NY 14263, Pamela.Hershberger@RoswellPark.org, Phone: 716-845-1697.

Disclosures: The authors have no conflicts of interest to disclose.

both compartments; and that the effect of CTA091 on tumor exposure was greater than its effect on plasma. These results provide evidence that CYP24-expressing lung tumors eliminate $1,25(OH)_2D_3$ by a CYP24-dependent process *in vivo* and that CTA091 administration represents a feasible approach to increase tumor exposure to $1,25(OH)_2D_3$.

Keywords

lung cancer; CTA091; CYP24; 1,25-dihydroxyvitamin D_3; pharmacokinetics

Introduction

The active metabolite of vitamin D_3, 1,25-dihydroxyvitamin D_3 ($1,25(OH)_2D_3$)1, exerts anti-proliferative activity by binding to the vitamin D receptor (VDR) and thereby regulating gene expression [1]. Recent studies suggest that $1,25(OH)_2D_3$ signaling inhibits the growth of established lung cancers. For example, $1,25(OH)_2D_3$ significantly inhibits the growth of some human lung cancer cell lines *in vitro* [2–4]. In other studies, serum levels of the $1,25(OH)_2D_3$ precursor 25-hydroxyvitamin D_3 ($25(OH)D_3$) were positively associated with survival in early-stage non-small cell lung cancer (NSCLC) patients [5], and high nuclear VDR levels in primary lung tumors were associated with significantly better overall survival [6]. Factors that reduce local $1,25(OH)_2D_3$ levels or signaling are predicted to support lung tumor growth and negatively impact patient outcome.

The mitochondrial P450 enzyme, 25-hydroxyvitamin D_3-24-hydroxylase (CYP24) is the predominant enzyme responsible for the catabolic inactivation of $1,25(OH)_2D_3$ [7]. CYP24 is frequently over-expressed in primary human lung tumors, where it may contribute to neoplastic growth by increasing the local elimination of $1,25(OH)_2D_3$ [8–10]. A pro-tumorigenic role for CYP24 is supported both by the recent discovery that *CYP24* mRNA expression is an independent predictor of poor survival in patients with lung adenocarcinoma [4], and by our prior finding that selective pharmacologic inhibition of CYP24 blocks $1,25(OH)_2D_3$ catabolism by lung cancer cells and increases its potency for growth inhibition *in vitro* [3]. The impact of tumor *CYP24* expression on the local elimination of $1,25(OH)_2D_3$ *in vivo* has not yet been determined.

Typically, *CYP24* transcription is increased by $1,25(OH)_2D_3$ in target tissues including the kidney, colon, intestine, and bone [11–13]. Physiologically, CYP24 may be induced by $1,25(OH)_2D_3$ to attenuate its action and prevent accumulation of toxic concentrations which would result in hypercalcemia. CYP24 induction is initiated when $1,25(OH)_2D_3$ binds to and activates the VDR. The activated receptor binds to vitamin D response elements (VDREs) located both within the *CYP24* promoter and downstream of the *CYP24* gene, resulting in robust transcriptional enhancement [14–16]. In mice lacking either the *VDR* gene or the *CYP24* gene, elevated blood levels of $1,25(OH)_2D_3$ were observed suggesting that VDR mediated induction of CYP24 is required for efficient $1,25(OH)_2D_3$ normalization [17–18].

Selective CYP24 inhibitors have been developed [19–22]. We hypothesize that these inhibitors may improve the efficacy of $1,25(OH)_2D_3$ for lung cancer treatment by increasing systemic exposure to $1,25(OH)_2D_3$ and preventing the local inactivation of $1,25(OH)_2D_3$ by lung tumors. It has not previously been possible to study the effects of CYP24 inhibition on $1,25(OH)_2D_3$ plasma *and* tumor pharmacokinetics (PK) due to the lack of a suitable assay for quantifying the active metabolite in a tumor matrix. To address this need, we developed

[1]**Abbreviations:** $1,25(OH)_2D_3$, 1,25-dihydroxyvitamin D_3; FBS, fetal bovine serum; GUS, β-glucuronidase; LC-MS/MS, liquid chromatography–tandem mass spectrometry; PK, pharmacokinetics; qPCR, quantitative PCR.

the liquid chromatography–tandem mass spectrometry (LC-MS/MS) assay reported in this paper. We used this assay to characterize $1,25(OH)_2D_3$ PK in the absence and presence of the CYP24 selective inhibitor, CTA091. CTA091 is a 24-sulfoximine analogue of $1,25(OH)_2D_3$ which binds to the substrate binding pocket of CYP24 and has previously been shown to increase plasma $1,25(OH)_2D_3$ exposure in rats [23–24].

In the H292 human lung tumor xenograft model, CTA091 significantly increased both the plasma *and* tumor C_{max} and AUC of co-administered $1,25(OH)_2D_3$. However, the increase in tumor exposure to $1,25(OH)_2D_3$ was not simply explained by a CTA091-mediated increase in plasma PK. Rather, our data suggest that lung tumors eliminate $1,25(OH)_2D_3$ *in vivo*, and that this local elimination may be preferentially inhibited via the use of CTA091. These findings suggest that CYP24 inhibitors may be useful in overcoming the deleterious effects of aberrant *CYP24* expression in human tumors. The assay we describe should be useful in addressing other clinically relevant questions about $1,25(OH)_2D_3$ pharmacokinetics.

Experimental

Chemicals and Reagents

$1,25(OH)_2D_3$ was purchased from Sigma-Aldrich (St. Louis, MO, USA). $[D_6]$-$1,25(OH)_2D_3$ (internal standard) was purchased from Medical Isotopes, Inc. (Pelham, NH). The CYP24 inhibitor CTA091 was generously provided by Cytochroma, Inc. (Markham, Ontario, Canada). For *in vitro* studies, CTA091 was used at a final concentration of 50 nM. At this concentration, CTA091 consistently and maximally inhibits $1,25(OH)_2D_3$ catabolism and significantly increases $1,25(OH)_2D_3$-mediated transcription (Zhang et al., manuscript under review). Methanol and water (HPLC grade) were purchased from Burdick and Jackson (Fombell, PA, USA). Methylene chloride, ammonium acetate and isopropanol (all HPLC grade) were purchased from Fisher Scientific (Fairlawn, NJ, USA). Nitrogen for evaporation of samples was purchased from Valley National Gases, Inc. (Pittsburgh, PA, USA). Nitrogen for mass spectrometrical applications was purified with a Parker Balston Nitrogen Generator (Parker Balston, Haverhill, MA, USA).

Cells

H292 human lung cancer cells were obtained from the American Type Culture Collection (Manassas, VA). H292 cells were maintained in RPMI 1640 supplemented with 10% fetal bovine serum (FBS) (HyClone Laboratories, Inc., Logan, UT), 2 mM L-glutamine, 10 mM HEPES, 1 mM sodium pyruvate, and 100 U/ml penicillin-streptomycin. Cells were maintained at 37°C in a humidified atmosphere containing 5% CO_2. The cell line was authenticated by RADIL (St. Louis, MO) and determined to be mycoplasma-free using the Venor GeM mycoplasma detection kit (Sigma Aldrich).

Quantitative PCR (qPCR)

RNA was isolated from H292 cells or tumor sections using the RNAgents system (Promega, Madison, WI) according to manufacturer's directions. The purified RNA was dissolved in nuclease-free water and quantitated by spectrophotometry at 260 nm. The integrity of each RNA preparation was confirmed by agarose gel electrophoresis. One μg of RNA was reverse-transcribed using random hexamer primers and MMLV reverse transcriptase for 1 h at 42 °C, as per instructions in the Advantage RT-for-PCR kit (Clontech Laboratories, Palo Alto, CA). The resulting cDNAs were diluted to a final volume of 100 μL in nuclease-free water. For qPCR, 2 μL of each cDNA were diluted in 1× Universal PCR Master Mix (Applied Biosystems, Branchburg, New Jersey) in a final volume of 30 μL with either a CYP24 primer/probe set (200 nM primer and 200 nM probe) or a β-glucuronidase (GUS)

primer/probe set (100 nM primer and 200 nM probe). The sequences of the CYP24 primers and probe were as follows: *Forward primer* 5'-CAT TTG GCT CTT TGT TGG ATT G; *Reverse primer* 5'-AGC ATC TCA ACA GGC TCA TTG TC; *Probe* 5'-/56-FAM-CCG CAA ATA CGA CAT CCA GGC CA-TAMRA. The GUS primer and probe sequences were from Herrera et al [25]. The qPCR reactions were run on an ABI 7700 sequence detection system (initial incubation at 95°C for 10 min followed by 40 cycles of 95°C for 15 sec, 60°C for 1 min) and the resulting data analyzed using Sequence Detection System software. Samples were assigned a Ct value for each gene (the cycle number at which the logarithmic PCR plots cross a fixed threshold). A CYP24 gene expression value (ΔCt) was calculated using the equation: ΔCt= [(Ct CYP24) – (Ct GUS)]. Linear mRNA expression values were obtained using the equation: mRNA expression = $2^{-\Delta Ct}$.

Tumor Xenografts

In vivo pharmacokinetic studies were conducted in 6–8 week old female *nu/nu* mice (Charles River Laboratories). Mice were housed in specific pathogen-free conditions according to the guidelines of the Association for the Assessment and Accreditation of Laboratory Animal Care, and studies were carried out under an approved institutional animal care and use protocol. Animals were housed in microisolator cages and provided food (Purina IsoPro Rodent 3000) and water *ad libitum*. Mice were fed the IsoPro diet upon their arrival and maintained on the same diet throughout the experiment. To establish xenografts, H292 cells in logarithmic growth (2.5×10^7 cells/mL) were mixed 1:1 with Matrigel (BD Biosciences). Two hundred μL of the suspension was injected subcutaneously into the left rear flank of each mouse. Once tumors developed, mice were stratified based on tumor volume to receive either $1,25(OH)_2D_3$ alone (20 μg/kg ip) or $1,25(OH)_2D_3$ (20 μg/kg ip) plus CTA091 (250 μg/kg ip). $1,25(OH)_2D_3$ and CTA091 were dissolved in absolute ethanol and diluted in sterile saline for injection. For all groups, the final injection volume was fixed at 0.1 mL, and the final ethanol concentration of the treatment stock was 12.5%. Groups of 2–7 animals were taken at pre-specified time points for pharmacokinetic analyses. Mice were euthanized by CO_2 inhalation, and blood was collected via cardiac puncture using heparinized syringes. Blood samples were stored on ice until all the samples for a given time point had been collected. Plasma was then prepared by centrifugation of the blood sample at 4 °C for 4 min, 13,000 × *g*. Tumors were excised and flash frozen in liquid nitrogen. Plasma and tumor were stored at −80 °C until analysis.

Preparation of $1,25(OH)_2D_3$ Standards

Stock solutions of $1,25(OH)_2D_3$ standards were prepared in methanol and stored at −80°C. Standard curves were prepared by diluting the stock solutions in plasma or H292 lung tumor homogenate (both from tumor-bearing, untreated female *nu/nu* mice). Tumors were homogenized in PBS (1:3, g/v) prior to use. $1,25(OH)_2D_3$ stocks were diluted into the appropriate matrix to achieve final concentrations ranging from 0.05 to 3 ng/mL (for tumor homogenate) or 0.1 to 100 ng/mL (for plasma).

Sample preparation

Sample preparation was performed on ice and in amber colored consumables when possible. To 200 μL of plasma or tumor homogenate were added 10 μL of internal standard (20 ng/mL of $[D_6]$-$1,25(OH)_2D_3$ in methanol/water, 50:50 (v/v)), and 1 mL of methylene chloride. The mixture was vortexed for 1 min. The vortexed sample was centrifuged for 6 min at 14,000 × g, after which the bottom layer was aspirated and evaporated to dryness under nitrogen at 37°C. After reconstitution of the dried residue in 500 μL of methylene chloride, the sample was subjected to solid phase extraction. An NH_2 Bond Elut Solid Phase Cartridge (200 mg, 3 mL, Varian Inc., Palo Alto, CA) was conditioned with 2 × 2 mL of methanol, and 2 mL of methylene chloride. The reconstituted sample was loaded and then

washed with 1 mL of methylene chloride and 1 mL of methylene chloride/isopropanol (98:2, v/v). The sample was eluted with 2 mL of methanol, evaporated to dryness under nitrogen at 37 °C, and reconstituted in 100 μL of mobile phase. The reconstituted sample was transferred to amber autosampler vials, and 50 μL was injected into the LC-MS/MS system.

Chromatography

The LC-MS/MS system consisted of an Agilent 1200 SL thermostated autosampler, binary pump with gradient. The liquid chromatography was performed with a gradient mobile phase consisting of A: methanol/2 mM ammonium acetate and B: 2 mM ammonium acetate. The mobile phase was pumped at a flow rate of 0.2 mL/min and separation was achieved using a Phenomenex (Torrance, CA) Synergi Hydro-RP column (4 μm, 100 × 2 mm) column. The gradient mobile phase was as follows: at time zero, solvent A was 80%, increased linearly to 99% in 8 min, and kept constant between 8 and 13 min. From 13 to 14 min, the percentage of solvent A was decreased linearly to 80%, while the flow rate was increased to 0.4 mL/min. This was maintained from 14 to 19.5 min, after which the flow rate was decreased to 0.2 mL/min between 19.5 and 20 min. The first 4 min of the column effluent were diverted to waste and the total run time was 20 min, with $1,25(OH)_2D_3$ eluting at approximately 12.5 min.

Mass spectrometric detection

Mass spectrometric detection was carried out using an MDS SCIEX 4000Q hybrid linear ion trap tandem mass spectrometer (MDS SCIEX, Concord, ON), with electrospray ionization operated in the positive mode, multiple reaction monitoring (MRM) mode. The settings of the mass spectrometer were as follows: curtain gas 20, IS voltage 5500 V, probe temperature 400 °C, GS1 40, GS2 30, declustering potential 50 V, collision energy 12 V. Quadrupoles were set to unit resolution and dwell time of 0.15 s. The MRM *m/z* transitions monitored for $1,25(OH)_2D_3$ and $[D_6]$-$1,25(OH)_2D_3$ were 434.5 to 399.5, and 440.5 to 405.4, respectively. The HPLC system and mass spectrometer were controlled by Analyst software (version 1.4.2), and data were collected with the same software. The analyte-to-internal standard ratio was calculated for each standard by dividing the area of each analyte peak by the area of the respective internal standard peak for that sample. Standard curves of the analytes were constructed by plotting the analyte-to-internal standard ratio *versus* the known concentration of analyte in each sample. Standard curves were fit by linear regression with weighting by $1/y^2$, followed by back calculation of concentrations.

Pharmacokinetic analysis and statistical interpretation

$1,25(OH)_2D_3$ concentration versus time data in plasma and tumor (averages per time point) were analyzed non-compartmentally using PK Solutions 2.0 (Summit Research Services, Montrose, CO; www.summitPK.com). The area under the plasma concentration versus time curve (AUC) was calculated with the linear trapezoidal rule for the period of observed data ($AUC_{0–8h}$), and the terminal elimination rate (k_e) was derived from the last, linear part of the data, followed by calculation of the half-life from $LN(2)/k_e$. Apparent clearance (Cl/F) was calculated as Dose/AUC, and apparent volume of distribution (V_d/F) was calculated as $(Cl/F)/k_e$.

Data were also analyzed compartmentally with the ADAPT 5 software for pharmacokinetic/pharmacodynamic systems analysis [26]. The maximum likelihood option in ADAPT 5 was used for all estimations (informed with the intercept and slope of the standard deviation versus concentration relationship obtained from the respective calibration curves) and model selection was based on Akaike's Information Criterion [27].

The effect of CTA091 on the elimination rates of $1,25(OH)_2D_3$ in plasma and in tumor was assessed by calculating the 95% confidence interval of these effects. Any effect characterized by a factor was considered significant if the 95% confidence interval did not include 1. Any effect characterized by a rate constant was considered significant if the 95% confidence interval did not include 0.

Results

$1,25(OH)_2D_3$ induces *CYP24* expression in H292 human lung cancer cells *in vitro* and *in vivo*

To study the effect of CYP24 on tumor elimination of $1,25(OH)_2D_3$ *in vivo*, we selected the H292 human lung tumor xenograft as our model system. When treated with $1,25(OH)_2D_3$ *in vitro*, H292 cells are induced to express *CYP24* (Fig. 1A). CYP24 induction is associated with the time-dependent loss of $1,25(OH)_2D_3$ from the culture system: only 20% of the initial dose remains 24 h post treatment (Fig. 1B). When H292 cells are exposed to $1,25(OH)_2D_3$ in the presence of the CYP24-selective inhibitor CTA091, >80% of the starting concentration of $1,25(OH)_2D_3$ remains after 24 h (Fig.1B). Although CTA091 alone has no effect on *CYP24* gene expression, it increases by approximately 4-fold the transcriptional induction of *CYP24* by $1,25(OH)_2D_3$ (data not shown). Cumulatively, these data support the conclusion that CTA091 effectively suppresses CYP24-mediated catabolism of $1,25(OH)_2D_3$ in H292 cells *in vitro*.

To determine whether $1,25(OH)_2D_3$ also increases *CYP24* expression in H292 cells *in vivo* (where it may contribute to tumor elimination of $1,25(OH)_2D_3$), we treated mice bearing established H292 xenografts with a single dose of $1,25(OH)_2D_3$. At various times thereafter, tumors were harvested and *CYP24* mRNA expression was assessed by qPCR. *CYP24* was expressed at low, but detectable levels immediately after $1,25(OH)_2D_3$ administration (Fig. 1C). *CYP24* mRNA levels were increased approximately 4-fold at 4 h post-treatment and nearly 15-fold after 8 h.

Development of an LC-MS/MS method for simultaneously quantitating $1,25(OH)_2D_3$ in plasma and tumor tissue

We developed an LC-MS/MS method that would allow for the absolute quantitation of $1,25(OH)_2D_3$ in plasma and tumor tissue (see Fig. 2 and details in Methods). Murine plasma obtained from a commercial source displayed high endogenous concentrations of $1,25(OH)_2D_3$ and was not suitable as the matrix for a $1,25(OH)_2D_3$ standard curve. Instead, standard curves were generated in plasma and tumor tissue homogenates that had been prepared from untreated tumor-bearing mice that were strain, age, and sex-matched to our experimental mice. The plasma and tumor homogenate assays were linear between 0.1–100 ng/mL $1,25(OH)_2D_3$ and 0.05–3 ng/mL $1,25(OH)_2D_3$, respectively. Assay performance was assessed in triplicate using samples that contained $1,25(OH)_2D_3$ at concentrations which spanned the dynamic range in each matrix (Table 1). The assay performed well in both matrices with accuracies between 87.3 and 110.7% and precisions within 2.9%. Extraction from each matrix was assessed by spiking 1 ng/mL $1,25(OH)_2D_3$ directly into plasma or tumor homogenate from untreated mice. Extraction from plasma was nearly complete at 92%, whereas extraction from tumor homogenate was much lower at 11.0%. CTA091 did not interfere with the detection of $1,25(OH)_2D_3$ (data not shown).

CYP24 contributes to the local elimination of $1,25(OH)_2D_3$ by lung tumors

To establish the effect of tumor *CYP24* expression on the elimination of $1,25(OH)_2D_3$ *in vivo*, mice bearing H292 subcutaneous xenografts were administered, via the intraperitoneal (i.p.) route, $1,25(OH)_2D_3$ alone (20 μg/kg) or $1,25(OH)_2D_3$ plus CTA091 (250 μg/kg).

Twenty μg/kg $1,25(OH)_2D_3$ was selected for use in these studies because it is a dose at which the plasma PK of $1,25(OH)_2D_3$ were previously characterized in a murine model using a different quantitative method [28]. The CTA091 dose was selected based on recommendations from the manufacturer and was expected to be biologically active given that a similar dose increased endogenous $1,25(OH)_2D_3$ levels and decreased serum PTH levels in rats [24]. In pilot studies, $1,25(OH)_2D_3$ and CTA091 could be co-administered at these doses without toxicity, and $1,25(OH)_2D_3$ concentrations in the linear range for detection in both plasma and tumor tissues were obtained (data not shown).

At various times post-treatment, blood and tumor tissue were collected for the determination of $1,25(OH)_2D_3$ by LC-MS/MS. The plasma pharmacokinetic profiles of $1,25(OH)_2D_3$ showed rapid absorption from the peritoneal cavity with a T_{max} of 0.25 h, followed by a first order elimination phase (Figure 3). Non-compartmental analysis indicated that the addition of the CYP24 inhibitor CTA091 increased the $1,25(OH)_2D_3$ plasma exposure approximately 1.5-fold, and the terminal half-life approximately 1.2-fold (Table 2). The tumor $1,25(OH)_2D_3$ concentration *versus* time profile was in accordance with that of a peripheral compartment, with T_{max}, at 2 h, lagging behind the plasma T_{max} of 0.25–0.5 h. Tumor concentrations were markedly lower than plasma concentrations, with an AUC ratio of tumor *versus* plasma of 13% and 22%, for $1,25(OH)_2D_3$ alone and with CTA091, respectively. The presence of CTA091 increased the tumor *versus* plasma ratio of the $1,25(OH)_2D_3$ AUC by a factor of approximately 1.8.

The plasma elimination rate constant (k_{l0}) for $1,25(OH)_2D_3$ and the apparent volume distribution (V_c/F) were estimated by compartmental analysis by fitting a one-compartment, open, linear model to the plasma $1,25(OH)_2D_3$ concentration *versus* time data (see model, Fig. 4). The half-life ($t_{1/2}$) of decline of $1,25(OH)_2D_3$ was calculated as $0.693/k_{10}$. Apparent clearance (Cl/F) was calculated as $(V_c/F)\bullet(k_{10})$. Next, an uncoupled tumor compartment was added to the model to be fit to the tumor concentration data. The uncoupled compartment approach allowed the concentration in the central compartment to drive entry to the tumor compartment and tumor concentration to drive loss from the tumor compartment, without having the amount of $1,25(OH)_2D_3$ in the central compartment being affected by these processes. The tumor volume was arbitrarily fixed at 1 L/kg. Next, the plasma and tumor $1,25(OH)_2D_3$ concentration data after co-administration of $1,25(OH)_2D_3$ and CTA091 were added to the dataset with the hypothesis that CTA091 could separately impact elimination of $1,25(OH)_2D_3$ from the central compartment (expressed as the factor Fp), and to inhibit elimination of $1,25(OH)_2D_3$ from the tumor (expressed as $k_{tumor\text{-}elim}$). The model fit the data well (Table 3), and the modest R^2 values merely reflect the variability in $1,25(OH)_2D_3$ concentration values among mice sampled at identical time points. Plasma pharmacokinetic parameters derived by non-compartmental and compartmental means were comparable. The factor by which the co-administration of CTA091 changed the elimination rate from the central compartment (F_p) was 0.805, and its 95% confidence interval did not include 1, thereby reaching significance. The elimination of $1,25(OH)_2D_3$ from the tumor which could be inhibited by co-administration of CTA091, independently from its effect on plasma exposure, was characterized by a rate constant $k_{tumor\text{-}elim}$ of 1.05 h^{-1}, with a 95% confidence interval that did not include 0, thereby also reaching significance.

Discussion

This is the first report of $1,25(OH)_2D_3$ concentrations in tumor xenografts, and how the plasma *and* tumor distribution of $1,25(OH)_2D_3$ can be increased independently by CTA091, a selective CYP24 inhibitor.

The $1,25(OH)_2D_3$ catabolizing enzyme CYP24 is expressed in normal tissues including the kidney [11], which affects $1,25(OH)_2D_3$ plasma pharmacokinetics, and in H292 tumors [Fig. 1], which may independently affect local tumor exposure to the steroid. Therefore, we hypothesized that CTA091 could separately impact the elimination of $1,25(OH)_2D_3$ from the central (plasma) compartment, and also inhibit elimination of $1,25(OH)_2D_3$ from the tumor itself. We indeed observed an increase in murine $1,25(OH)_2D_3$ plasma AUC and C_{max} of 1.5 and 1.6-fold, respectively, after co-administration of CTA091 and $1,25(OH)_2D_3$, which agrees with a previously reported increase in rat serum $1,25(OH)_2D_3$ exposure and C_{max} of 1.4-fold and 1.5-fold, respectively, after 500 μg/kg CTA091 [24]. A similar effect of pharmacologic CYP24 inhibition on $1,25(OH)_2D_3$ plasma PK was observed in studies conducted by Muindi *et al* [28]: Co-administration of $1,25(OH)_2D_3$ with ketoconazole, a general inhibitor of P450 enzymes including CYP24, resulted in a 1.3-fold increase in $1,25(OH)_2D_3$ serum AUC. We build upon this prior work by demonstrating that tumors which express *CYP24* eliminate $1,25(OH)_2D_3$ *in vivo*, and that an additional consequence of systemic pharmacologic CYP24 inhibition appears to be the preferential suppression of local tumor-mediated catabolism of $1,25(OH)_2D_3$.

The higher ratio of tumor *versus* plasma AUC of $1,25(OH)_2D_3$ in the presence of CYP24 inhibitor CTA091 suggests that CTA091 has an effect on the tumor disposition of $1,25(OH)_2D_3$ independent of its effect on the plasma disposition (Table 2). By compartmental modeling, we were able to derive $1,25(OH)_2D_3$ pharmacokinetic parameters and parameters to quantitate the effects of CTA091 on $1,25(OH)_2D_3$ pharmacokinetics (Table 3). CTA091 administration resulted in a significant 20% decrease in plasma clearance of $1,25(OH)_2D_3$ ($K_{10}*F_p/k_{10} = 0.81$) and a significant 46% decrease in tumor clearance ($k_{tc}/(k_{tc}+ k_{tumor\ elim}) = 0.54$). Thus, the effect of CTA091 on tumor $1,25(OH)_2D_3$ exposure is larger than its effect on plasma $1,25(OH)_2D_3$ exposure. This may be explained by the pharmacokinetics of CTA091 itself, which is cleared from plasma more rapidly than $1,25(OH)_2D_3$ (personal communication, M. Petkovich). Retention of CTA091 in tumor may therefore prolong the local CYP24 inhibition, while systemically, the CYP24 inhibition is likely to be shorter and less pronounced. This also highlights that the currently applied compartmental model, which assumes a constant inhibitory effect of CTA091 on CYP24, is an oversimplification. However, only with more detailed information about CTA091 disposition can the model be further refined. Next generation CYP24 inhibitors should be designed to be metabolically more stable, which will allow for more durable increases of $1,25(OH)_2D_3$ tissue exposure. Alternatively, $1,25(OH)_2D_3$ exposure may be increased by repeated dosing of a less stable CYP24 inhibitor.

Theoretically, CTA091 treatment could have instead resulted in a preferential increase in $1,25(OH)_2D_3$ levels in tumors because it induced local expression of the $1,25(OH)_2D_3$-synthesizing enzyme, *CYP27B1*. To explore this possibility, we did examine the effect of CTA091 treatment on *CYP27B1* mRNA expression. *CYP27B1* is expressed at very low, but detectable levels in H292 cells. CTA091 alone had no effect on expression *in vitro*, nor was *CYP27B1* modulated in cells treated with $1,25(OH)_2D_3$ plus CTA091 (data not shown). These negative findings lend further support to the notion that CTA091 exerts its effects in the H292 xenograft model through CYP24 –mediated inhibition of $1,25(OH)_2D_3$ catabolism rather than through the stimulation of $1,25(OH)_2D_3$ production. A different result could be obtained in a tumor model system which expresses higher basal levels of CYP27B1. In this setting, since CYP24 also acts on the CYP27B1 substrate ($25(OH)D_3$), CYP24 inhibition with CTA091 would be predicted to support endogenous, local hormone production.

In prior studies of $1,25(OH)_2D_3$ plasma pharmacokinetics in non-tumor bearing C3H/HeJ mice, hormone concentrations were determined by radioimmunoassay (RIA) following a bolus *ip* dose of $1,25(OH)_2D_3$. The $1,25(OH)_2D_3$ Cmax and AUC that were calculated by

Muindi *et al*. [28] are approximately 2-fold higher than those determined in our current study, despite the administration of the same dose of $1,25(OH)_2D_3$ by the same route. The differences may reflect a relative increase in the catabolism of $1,25(OH)_2D_3$ in *nu/nu* mice compared to C3H/HeJ mice. Significant interstrain differences in vitamin D_3 metabolism have been described previously [29].

In its current configuration, the LC-MS/MS plasma assay we developed has a lower limit of quantitation of 100 pg/mL $1,25(OH)_2D_3$ and does not detect endogenous levels of $1,25(OH)_2D_3$ in plasma of *nu/nu* mice. Literature reported values of serum $1,25(OH)_2D_3$ in untreated mice range from 40 pg/mL in BALB/c mice to 80 pg/mL in C3H/HeJ mice [28–29]. If the baseline serum biochemistry of the mice we used is similar to these, it is not surprising that endogenous $1,25(OH)_2D_3$ levels were not detected. Nonetheless, our assay could be used to provide new information on $1,25(OH)_2D_3$ plasma *and* tumor pharmacokinetics following exogenous administration. For example, we are the first to quantify intratumoral concentrations of $1,25(OH)_2D_3$. Tumor concentrations reached a maximum of 1.7 ng/g $1,25(OH)_2D_3$ in the absence of CTA091 and 4.43 ng/g in its presence. Given that 1 g of tumor has a volume of 1 mL, peak tumor concentrations of 3.8 nM and 10 nM $1,25(OH)_2D_3$ were achieved without or with CTA091, respectively.

Clinical trials show that $1,25(OH)_2D_3$ alone can be safely delivered at high doses (0.5 μg/kg) on a once weekly basis in the oncology setting [30]. It remains to be determined whether single agent $1,25(OH)_2D_3$ (at its maximally tolerated dose) will result in a lower tumor exposure than is achieved by combining $1,25(OH)_2D_3$ with a CYP24 inhibitor (at their maximally tolerated doses) and whether this will translate into meaningful differences in anti-tumor efficacy. The impact of variation in *CYP24* expression level on tumor exposure to $1,25(OH)_2D_3$ also remains to be determined. The LC-MS/MS assay described here will be utilized in the future to address these clinically relevant questions.

Highlights

- The vitamin D_3 catabolizing enzyme, CYP24, is over-expressed in lung tumors.
- To study tumor catabolism of vitamin D_3, an LC-MS/MS assay was developed.
- Assay results show that lung tumor xenografts locally eliminate vitamin D_3.
- A CYP24 inhibitor independently increased plasma and tumor exposure to vitamin D_3.
- CYP24 inhibition is a feasible approach to increase tumor exposure to vitamin D_3.

Acknowledgments

We wish to thank Dr. Julie Eiseman (University of Pittsburgh) for many helpful discussions, Ms. Natalie Alexander for assistance with animal studies, and the University of Pittsburgh Cancer Institute Writing Group for reviewing an early version of this manuscript. We also wish to acknowledge the scientific contributions and enthusiastic support of our mentor and friend, Dr. Merrill Egorin, who passed away before this work could be completed. This work was supported by R01 CA132844 to PAH. This project used the UPCI Clinical Pharmacology Analytical Facility and was supported in part by award P30CA047904.

References

1. Deeb KK, Trump DL, Johnson CS. Vitamin D signalling pathways in cancer: potential for anticancer therapeutics. Nat Rev Cancer. 2007; 7(9):684–700. [PubMed: 17721433]

2. Guzey M, Sattler C, DeLuca HF. Combinational effects of vitamin D_3 and retinoic acid (all trans and 9 cis) on proliferation, differentiation, and programmed cell death in two small cell lung carcinoma cell lines. Biochem Biophys Res Commun. 1998; 249(3):735–744. [PubMed: 9731207]
3. Parise RA, Egorin MJ, Kanterewicz B, Taimi M, Petkovich M, Lew AM, et al. CYP24, the enzyme that catabolizes the antiproliferative agent vitamin D, is increased in lung cancer. Int J Cancer. 2006; 119(8):1819–1828. [PubMed: 16708384]
4. Chen G, Kim SH, King AN, Zhao L, Simpson RU, Christensen PJ, et al. CYP24A1 is an independent prognostic marker of survival in patients with lung adenocarcinoma. Clin Cancer Res. 2011; 17(4):817–826. [PubMed: 21169243]
5. Zhou W, Heist RS, Liu G, Asomaning K, Neuberg DS. Circulating 25-hydroxyvitamin D levels predict survival in early-stage non-small-cell lung cancer patients. J Clin Oncol. 2007; 25(5):479–485. [PubMed: 17290055]
6. Srinivasan M, Parwani AV, Hershberger PA, Lenzner DE, Weissfeld JL. Nuclear vitamin D receptor expression is associated with improved survival in non-small cell lung cancer. J Steroid Biochem Mol Biol. 2011; 123(1–2):30–36. [PubMed: 20955794]
7. Prosser DE, Jones G. Enzymes involved in the activation and inactivation of vitamin D. Trends Biochem Sci. 2004; 29(12):664–673. [PubMed: 15544953]
8. Beer DG, Kardia SL, Huang CC, Giordano TJ, Levin AM, Misek DE, et al. Gene-expression profiles predict survival of patients with lung adenocarcinoma. Nat Med. 2002; 8(8):816–824. [PubMed: 12118244]
9. Anderson MG, Nakane M, Ruan X, Kroeger PE, Wu-Wong JR. Expression of VDR and CYP24A1 mRNA in human tumors. Cancer Chemother Pharmacol. 2006; 57:234–240. [PubMed: 16180015]
10. Kim B, Lee HJ, Choi HY, Shin Y, Nam S, Seo G. Clinical validity of the lung cancer biomarkers identified by bioinformatics analysis of public expression data. Cancer Res. 2007; 67(15):7431–7438. [PubMed: 17671213]
11. Reddy SG, Tserng K. Calcitroic acid, end product of renal metabolism of 1,25-dihydroxyvitamin D_3 through C-24 oxidation pathway. Biochemistry. 1989; 28:1763–1769. [PubMed: 2719932]
12. Tomon M, Tenenhouse HS, Jones G. 1,25-Dihydroxyvitamin D_3-inducible catabolism of vitamin D metabolites in mouse intestine. Am J Physiol. 1990; 258(4 Pt 1):G557–G563. [PubMed: 2159220]
13. Henry HL. The $25(OH)D_3$/1α,$25(OH)_2D_3$-24R-hydroxylase: a catabolic or biosynthetic enzyme? Steroids. 2001; 66:391–398. [PubMed: 11179748]
14. Chen KS, DeLuca HF. Cloning of the human 1α,25-dihydroxyvitamin D_3 24-hydroxylase gene promoter and identification of two vitamin D-responsive elements. Biochim. Biophys. Acta. 1995; 1263:1–9. [PubMed: 7632726]
15. Ohyama Y, Ozono K, Uchida M, Yoshimura M, Shinki T, Suda T, et al. Functional assessment of two vitamin D-responsive elements in the rat 25-hydroxyvitamin D_3 24-hydroxylase gene. J Biol Chem. 1996; 271:30381–30385. [PubMed: 8940000]
16. Meyer MB, Goetsch PD, Pike JW. A downstream intergenic cluster of regulatory enhancers contributes to the induction of CYP24A1 expression by 1α,25-dihydroxyvitamin D_3. J Biol Chem. 2010; 285(20):15599–15610. [PubMed: 20236932]
17. Endres B, Kato S, DeLuca HF. Metabolism of 1α,25-Dihydroxyvitamin D_3 in Vitamin D Receptor-Ablated Mice in Vivo. Biochemistry. 2000; 39:2123–2129. [PubMed: 10684662]
18. Masuda S, Byford V, Arabian A, Sakai Y, Demay MB, St-Arnaud R, et al. Altered pharmacokinetics of 1,α,25-dihydroxyvitamin D_3 and 25-hydroxyvitamin D_3 in the blood and tissues of the 25-hydroxyvitamin D-24-Hydroxylase (Cyp24a1) Null Mouse. Endocrinology. 2005; 146:825–834. [PubMed: 15498883]
19. Schuster I, Egger H, Bikle D, Herzig G, Reddy GS, Stuetz A, et al. Inhibitors of vitamin D hydroxylases: structure-activity relationships. J Cell Biochem. 2003; 88(2):372–380. [PubMed: 12520539]
20. Yee SW, Simons C. Synthesis and CYP24 inhibitory activity of 2-substituted-3,4-dihydro-2Hnaphthalen- 1-one (tetralone) derivatives. Bioorg Med Chem Lett. 2004; 14(22):5651–5654. [PubMed: 15482941]

21. Posner GH, Crawford KR, Yang HW, Kahraman M, Jeon HB, Li H, et al. Potent, low-calcemic, selective inhibitors of CYP24 hydroxylase: 24-sulfone analogs of the hormone 1α,25-dihydroxyvitamin D_3. J Steroid Biochem Mol Biol. 2004; 89–90(1–5):5–12.
22. Schuster I, Egger H, Herzig G, Reddy GS, Schmid JA, Schussler M, et al. Selective inhibitors of vitamin D metabolism--new concepts and perspectives. Anticancer Res. 2006; 26(4A):2653–2668. [PubMed: 16886676]
23. Kahraman M, Sinishtaj S, Dolan PM, Kensler TW, Peleg S, Saha U, et al. Potent, selective and low-calcemic inhibitors of CYP24 hydroxylase: 24-sulfoximine analogues of the hormone 1α,25-dihydroxyvitamin D_3. J Med Chem. 2004; 47(27):6854–6863. [PubMed: 15615534]
24. Posner GH, Helvig C, Cuerrier D, Collop D, Kharebov A, Ryder K, et al. Vitamin D analogues targeting CYP24 in chronic kidney disease. J Steroid Biochem Mol Biol. 2010; 121(1–2):13–19. [PubMed: 20347976]
25. Herrera LJ, El-Hefnawy T, Queiroz de Oliveira PE, Raja S, Finkelstein S, Gooding W, et al. The HGF receptor c-Met is overexpressed in esophageal adenocarcinoma. Neoplasia. 2005; 7(1):75–84. [PubMed: 15720819]
26. D'Argenio, DZ.; Scumitzky, A. ADAPT II user's guide: pharmacokinetic/pharmacodynamic systems analysis software. Los Angeles: University of Southern California; 1997.
27. Akaike H. A Bayesian extension of the minimal AIC procedures of autoregressive model fitting. Biometrika. 1979; 66:237–242.
28. Muindi JR, Modzelewski RA, Peng Y, Trump DL, Johnson CS. Pharmacokinetics of 1α,25-dihydroxyvitamin D_3 in normal mice after systemic exposure to effective and safe antitumor doses. Oncology. 2004; 66:62–66. [PubMed: 15031600]
29. Misharin A, Hewison M, Chen CR, Lagishetty V, Aliesky HA, Mizutori Y. Vitamin D deficiency modulates Graves' hyperthyroidism induced in BALB/c mice by thyrotropin receptor immunization. Endocrinology. 2009; 150(2):1051–1060. [PubMed: 18927213]
30. Beer TM, Munar M, Henner WD. A Phase I Trial of Pulse Calcitriol in Patients with Refractory Malignancies. Cancer. 2001; 91:2431–2439. [PubMed: 11413535]

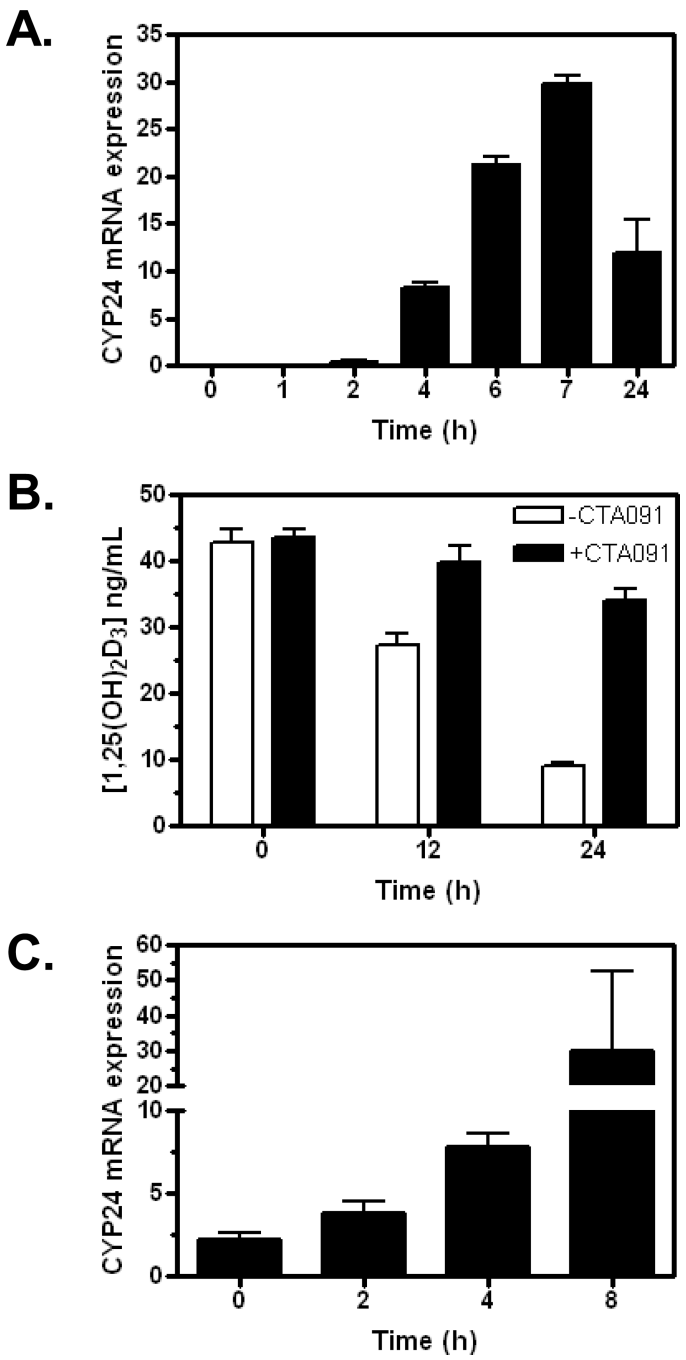

Figure 1.

H292 cells express CYP24 *in vitro* and *in vivo*. (A) H292 cells were treated with 1 nM $1,25(OH)_2D_3$. At the times indicated, cells were harvested and RNA was prepared. *CYP24* mRNA expression was determined by QPCR, as detailed in methods. Results are the average of two separate determinations. (B) H292 cells were exposed to 100 nM $1,25(OH)_2D_3$ in the absence (white bars) or presence (black bars) of CTA091 (50 nM). At various times, tissue culture homogenates were prepared and $1,25(OH)_2D_3$ concentrations determined by LC-MS/MS. Values represent the mean +/− SD for triplicate determinations. (C) Mice bearing H292 xenografts were treated with a single dose of $1,25(OH)_2D_3$. At various times, tumors were harvested for determination of *CYP24* mRNA levels by QPCR.

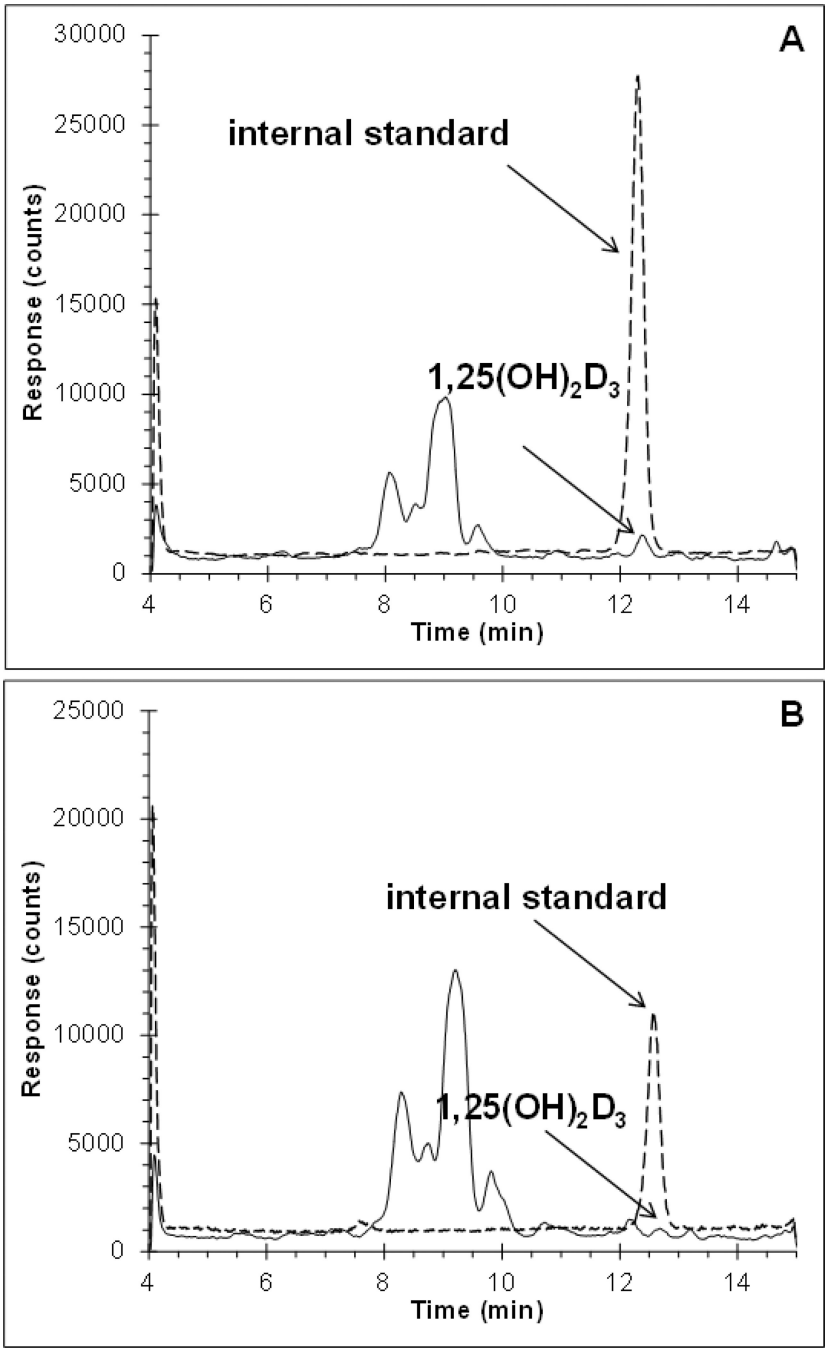

Figure 2.
Chromatograms of $1,25(OH)_2D_3$ (eluting at 12.5 min) at the lower limit of quantitation of (A) mouse plasma at 0.1 ng/mL, and (B) tumor homogenate at 0.05 ng/mL ($1,25(OH)_2D_3$, continuous line; internal standard, dashed line with an offset of +500).

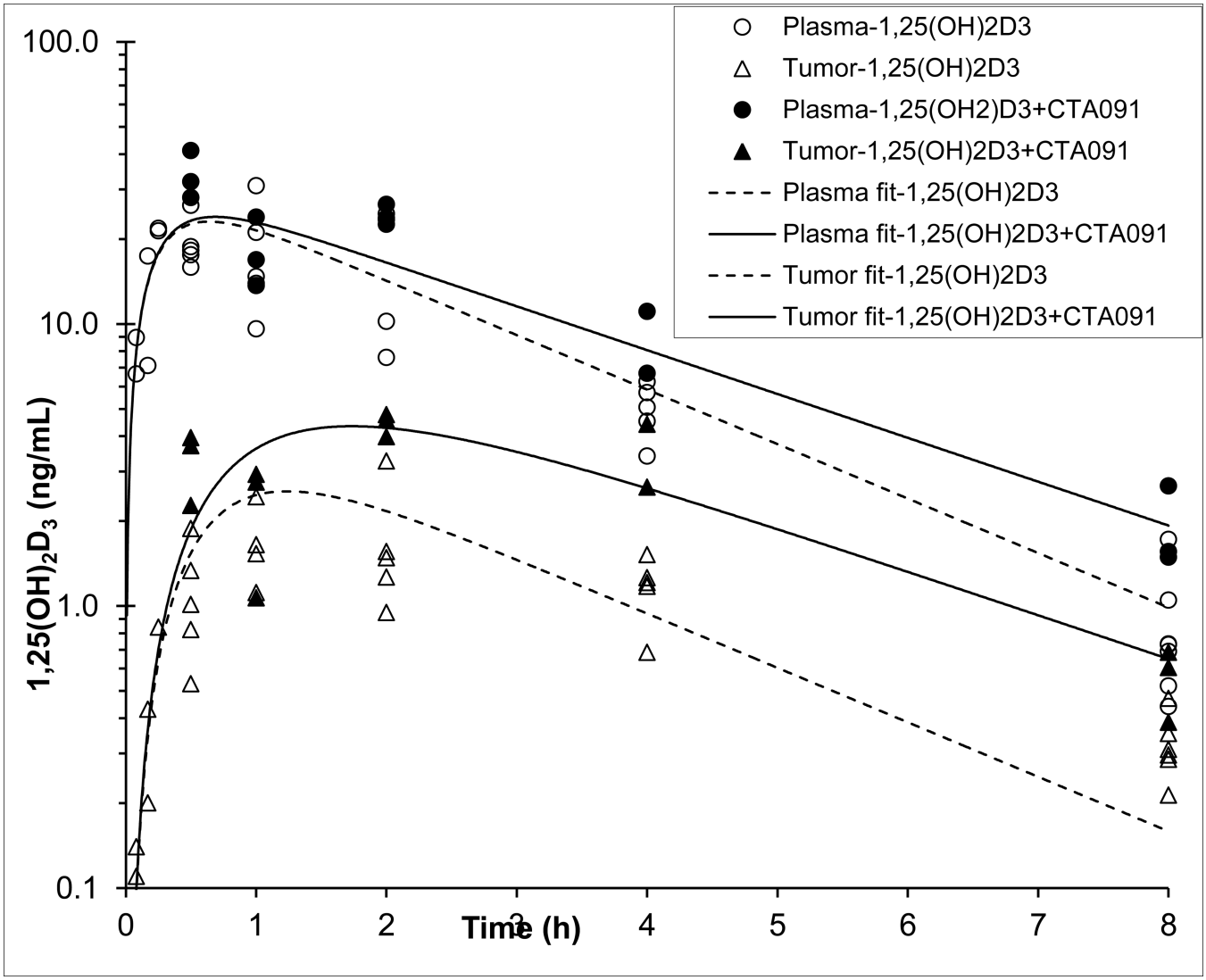

Figure 3.

Concentration versus time data and model fits of $1,25(OH)_2D_3$ in plasma (circles) and tumor (triangles) after i.p. administration to tumor-bearing nu/nu mice of 20 μg/kg $1,25(OH)_2D_3$ either alone (open symbols, dashed lines) or in combination with 250 μg/kg of the CYP24 inhibitor, CTA091 (solid symbols, solid lines).

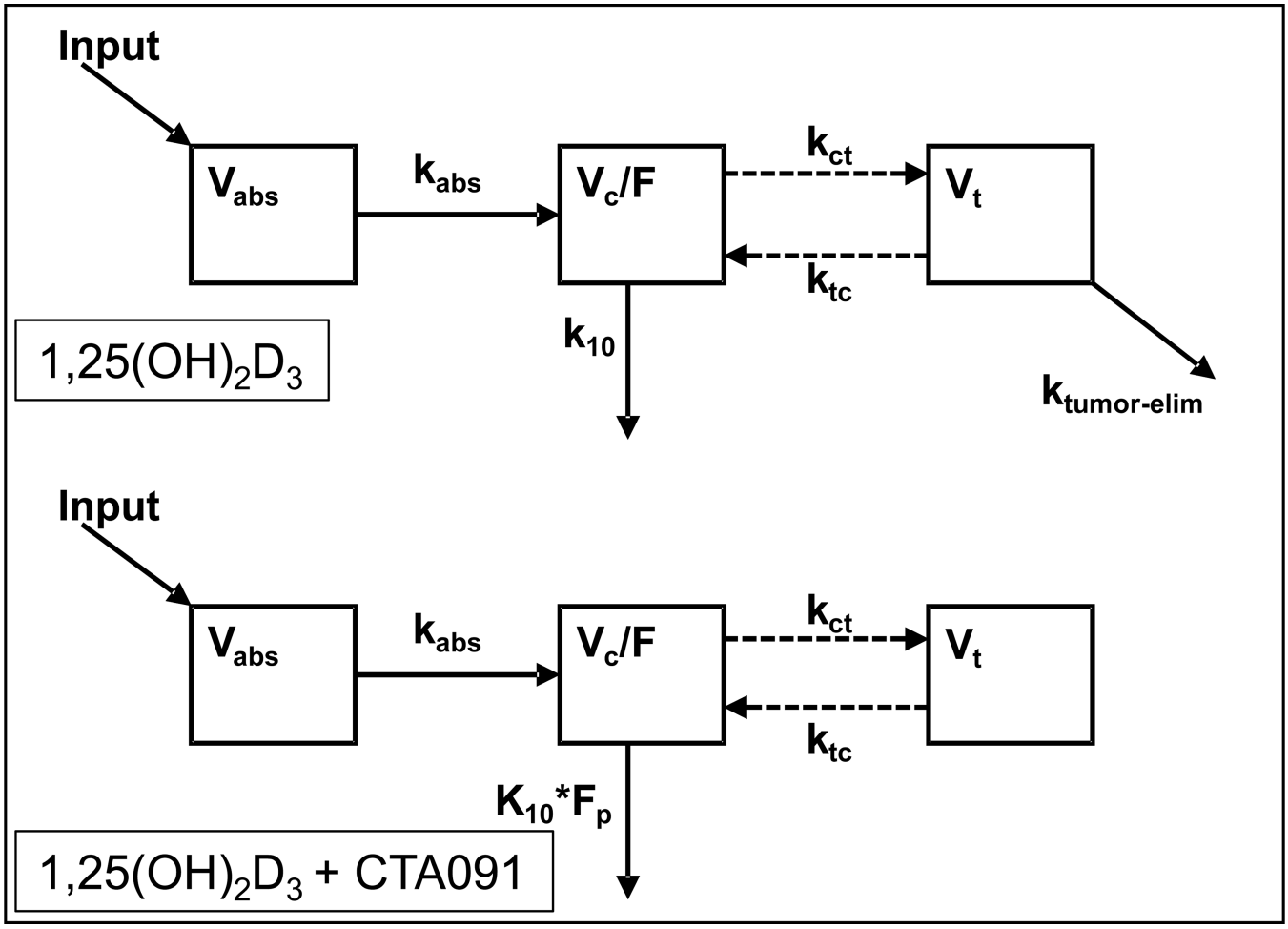

Figure 4.

Model structure used to estimate pharmacokinetic parameters of $1,25(OH)_2D_3$ in plasma and tumors. Note how the co-administration of CTA091 is hypothesized to both impact elimination of $1,25(OH)_2D_3$ from the central compartment (F_p), and to inhibit elimination of $1,25(OH)_2D_3$ from the tumor ($k_{tumor-elim}$).

Table 1

Assay performance parameters at representative points along the dynamic range.

[1,25(OH)$_2$D$_3$] (ng/mL)	Accuracy (%)	Precision (%)	Recovery (%)
Plasma			
0.1	95.0	2.5	-
1.0	110.7	1.9	92.2 (11.4)
10	97.4	0.4	-
100	87.3	2.1	-
Tumor homogenate			
0.1	110.7	2.9	-
0.3	105.0	2.6	-
1.0	89.6	0.8	11.0 (16.1)
3.0	96.3	1.2	-

Assay performance was assessed in triplicate using samples that contained the indicated concentrations of 1,25(OH)$_2$D$_3$. Precision was calculated as the relative standard deviation. Accuracy was calculated as the back-calculated concentration relative to the nominal concentration. Extraction recovery was assessed at 1 ng/mL 1,25(OH)$_2$D$_3$ and was calculated as the relative response of an extracted sample *versus* the response of a standard in mobile phase.

Table 2

Results of the non-compartmental analysis of plasma and tumor $1,25(OH)_2D_3$ concentration versus time data.

Parameter	Unit	$1,25(OH)_2D_3$	$1,25(OH)_2D_3$ + CTA091	+/− CTA091 Ratio
Plasma				
$AUC_{0–8h}$	ng/mL•h	67.4	97.3	1.4
$AUC_{0\text{-}inf}$	ng/mL•h	69.1	102	1.5
C_{max}	ng/mL	21.6	33.7	1.6
T_{max}	h	0.25	0.5	2
V_d/F	L/kg	0.592	0.469	0.79
K_{el}	h^{-1}	0.489	0.419	0.86
$t_{1/2}$	h	1.42	1.66	1.2
Cl/F	L/h/kg	0.289	0.196	0.68
Tumor				
$AUC_{0–8h}$	ng/g•h	8.39	21.7	2.6
$AUC_{0\text{-}inf}$	ng/g•h	9.18	22.9	2.5
C_{max}	ng/g	1.70	4.43	2.6
T_{max}	h	2	2	1
k_{el}	h^{-1}	0.355	0.460	1.3
$t_{1/2}$	h	1.95	1.51	0.77
Tumor/plasma				
$AUC_{0–h}$	-	0.125	0.22	1.8
C_{max}	-	0.079	0.13	1.7

Concentration versus time data were obtained after i.p. administration of 20 μg/kg $1,25(OH)_2D_3$ either alone or in combination with 250 μg/kg of CTA091 to mice bearing subcutaneous H292 lung tumors. $AUC_{0–8h}$, area under the concentration *versus* time curve from 0 to 8 h; $AUC_{0\text{-}inf}$, area under the concentration *versus* time curve from 0 to infinity; C_{max}, maximum concentration; T_{max}, time of C_{max}; V_d/F, apparent volume of distribution; k_{el}, elimination rate constant; $t_{½}$, half-life; Cl/F, apparent clearance.

Table 3

Results of the compartmental analysis of plasma and tumor $1,25(OH)_2D_3$ concentration versus time data

		$1,25(OH)_2D_3$	
Parameter	**Unit**	**Estimate (%SE)**	**95%-CI**
Plasma			
k_a	h^{-1}	3.82 (19)	2.36–5.28
V_c/F	L/kg	0.653 (8.4)	0.543–0.763
k_{10}	h^{-1}	0.445 (5.3)	0.398–0.491
F_p	-	0.805 (7.1)	0.691–0.919
Cl/F_$1,25(OH)_2D_3$	L/h/kg	0.291 (6.1)	0.255–0.326
Cl/F_$1,25(OH)_2D_3$+CTA091	L/h/kg	0.234 (7.7)	0.198–0.270
t½_$1,25(OH)_2D_3$	h	1.56 (5.3)	1.40–1.72
t½_$1,25(OH)_2D_3$+CTA091	h	1.94 (7.6)	1.65–2.23
R^2_$1,25(OH)_2D_3$	-	0.695	
R^2_$1,25(OH)_2D_3$+CTA091	-	0.702	
Tumor			
V_t	L/kg	1 (not estimated)	-
k_{ct}	h^{-1}	0.454 (18)	0.287–0.620
k_{tc}	h^{-1}	1.24 (22)	0.687–1.79
$k_{tumor\text{-}elim}$	h^{-1}	1.04 (32)	0.371–1.72
$t½_{\text{–tumor-elim}}$	h	0.661 (32)	0.236–1.09
R^2_$1,25(OH)_2D_3$	-	0.569	
R^2_$1,25(OH)_2D_3$+CTA091	-	0.447	
AIC	-	332.5	

Data were obtained after i.p. administration of 20 μg/kg $1,25(OH)_2D_3$ either alone or in combination with 250 μg/kg of the CYP24 inhibitor CTA091 to mice bearing subcutaneous H292 lung tumors. K_a, absorption rate constant; V_c/F, apparent central volume of distribution; K_{10}, $1,25(OH)_2D_3$ elimination rate constant from the central compartment; F_p, factor by which CTA091 changes the elimination of $1,25(OH)_2D_3$ from the central compartment; Cl/F, apparent clearance; $t_{½}$, half-life; R^2, correlation coefficient; V_t, tumor volume; k_{ct}, $1,25(OH)_2D_3$ transfer rate constant from the central to the tumor compartment; k_{tc}, $1,25(OH)_2D_3$ transfer rate constant from the tumor to the central compartment; $k_{tumor\text{-}elim}$, $1,25(OH)_2D_3$ elimination rate constant from the tumor compartment that is inhibited with CTA091; AIC, Akaike's Information Criterion.